Article

On the Comparison of Flow Physics between Minimal and Extended Flow Units in Turbulent Channels

Ethan A. Davis [†] ⬤, Siamak Mirfendereski [†] ⬤ and Jae Sung Park * ⬤

Department of Mechanical and Materials Engineering, University of Nebraska-Lincoln,
Lincoln, NE 68588-0526, USA; ethan.davis@huskers.unl.edu (E.A.D.); siamak.mir@huskers.unl.edu (S.M.)
* Correspondence: jaesung.park@unl.edu
† These authors contributed equally to this work.

Abstract: Direct numerical simulations were performed to study the effects of the domain size of a minimal flow unit (MFU) and its inherent periodic boundary conditions on flow physics of a turbulent channel flow in a range of $200 \leq Re_\tau \leq 1000$. This was accomplished by comparing turbulent statistics with those computed in sub-domains (SD) of extended domain simulations. The dimensions of the MFU and SD were matched, and SD dynamics were set to minimize artificial periodicities. Streamwise and spanwise dimensions of healthy MFUs were found to increase linearly with Reynolds number. It was also found that both MFU and SD statistics and dynamics were healthy and in good agreement. This suggests that healthy MFU dynamics represent extended-domain dynamics well up to $Re_\tau = 1000$, indicating a nearly negligible effect of periodic conditions on MFUs. However, there was a small deviation within the buffer layer for the MFU at $Re_\tau = 200$, which manifested in an increased mean velocity and a tail in the Q2 quadrant of the u'-v' plane. Thus, it should be noted that when considering an MFU domain size, stricter criteria may need to be put in place to ensure healthy turbulent dynamics.

Keywords: turbulence; flow physics; direct numerical simulation; minimal flow units; extended flow units

1. Introduction

Embedded in a turbulent flow is inherent intermittency. The dynamics of wall-bounded turbulence fluctuate between high, intermediate, and low-drag states in a stochastic fashion, which illuminates the self-sustaining process in shear flows [1–4]. The most straightforward simulation approach to identify the intermittency and self-sustaining structures is the so-called minimal flow unit (MFU) approach [5]. A minimal flow unit is the smallest simulation domain for a given set of parameters, such as Reynolds numbers, containing the essential self-sustaining elements for which turbulence persists. In MFUs, turbulent statistics are spatially correlated, indicating that the entire domain completely experiences the same dynamics. Accordingly, temporally intermittent phenomena can be readily identified by spatial averaging. Thus, the MFU dynamics allow one to concentrate only on the temporal intermittency of turbulence. However, it should be noted that an MFU should at least maintain "healthy" near-wall turbulence that reproduces the self-sustaining process and statistical characteristics of full turbulence [6–9]. In particular, an MFU should be able to contain a single ejection and sweep event by which streamwise streaks and vortices are sustained [10].

In an extended domain, turbulent statistics become less correlated in space and the intermittency becomes both spatial and temporal in nature. In this situation, spatially-averaged statistics could mix information together from different regions, which makes identification of spatiotemporal intermittency difficult to recognize. Moreover, the effects of the computational domain size on turbulent dynamics could be profound [11]. In addition, as the Reynolds number increases, the spatiotemporal intermittency becomes more

noticeable [12–14]. A natural question is how closely the MFU dynamics are related to the spatiotemporal intermittency in a spatially extended domain. This extended domain can be thought of as a more experimentally realizable flow for which no artificial periodicities are imposed [15]. There have been studies to draw the links between minimal-domain temporal intermittency and extended-domain spatiotemporal intermittency for the transitional Reynolds number regime [15,16], but it has yet to be explored for higher Reynolds numbers until now, which is a focus of the present work.

Prior to proceeding to the present work, we aim to provide a brief description of the minimal flow unit and its potential connection to William W. Willmarth's legacy in turbulent flows. Direct numerical simulations (DNSs) based on minimum flow units have been extensively performed for a variety of purposes, including understanding near-wall turbulent dynamics [17–20] and flow control [21–23]. A minimum flow unit involves the periodic computational domain, which has the minimum spanwise length of approximately 100 wall units and the minimum streamwise length of approximately 250–350 wall units [5]. Interestingly, an MFU with the minimum lengths could capture the turbulence intensity at the near-wall in a turbulent channel experiment performed by Wei and Willmarth [24]. However, lengths too small to accommodate the large-scale structure are likely to result in a statistical abnormality and minimal log layer in a mean velocity [5]. Although the outer portion of the boundary layer might not significantly influence the inner-layer statistics to some extent [25], the influence of the outer layer flow on near-wall flow structures becomes important when there is a significant cancellation in the logarithmic layer. Thus, it is worth noting that the deterioration of near-wall turbulence with narrow MFU domains for higher Reynold numbers could result in the disappearance of the logarithmic region in the mean velocity profile. This situation can be referred to as "unhealthy" turbulence. As mentioned above, ejection and sweep events should be accommodated for valid MFU dynamics. These events could be related to Reynolds stress and coherent structures by means of the so-called quadrant analysis. This approach was advanced by Willmarth and Lu [26–29]. This quadrant analysis will be employed in the current study to draw connections between MFU dynamics and extended-domain dynamics.

This paper is organized as follows. Section 2 presents the problem formulation and numerical details for the current study. In Section 3, we present the size of minimal flow units and compare MFU statistics and dynamics to ones for a sub-domain of the same size embedded in an extended domain, for which quadrant analysis was employed. Finally, a summary and implications of the present investigation are given in Section 4.

2. Problem Formulation

We consider a direct numerical simulation (DNS) of an incompressible Newtonian fluid in the plane Poiseuille (channel) geometry, driven by constant volumetric flux Q. The domain was aligned such that the x, y, and z coordinates corresponded to the streamwise, wall-normal, and spanwise directions, respectively. For all DNSs, periodic boundary conditions were imposed in the x and z directions with the maximum wavelengths of L_x and L_z, and a no-slip boundary condition was imposed at the top and bottom walls $y = \pm h$, where $h = L_y/2$ is the channel half-height. However, data analyzed from the extended domain DNS were taken from a sub-domain (SD) which matches the fundamental periods of the MFU, namely, L_x and L_z. An SD was located in the middle of the extended domain to minimize any potential artificial effects of periodic boundaries. The laminar centerline velocity for a given volumetric flux is given by $U_{cl} = (3/4)Q/h$. Using the channel half-height h and the laminar centerline velocity U_{cl} as the characteristic length and velocity scales, the non-dimensionalized continuity and Navier-Stokes equations are given as

$$\nabla \cdot \boldsymbol{u} = 0, \tag{1}$$

$$\frac{\partial \boldsymbol{u}}{\partial t} + \boldsymbol{u} \cdot \nabla \boldsymbol{u} = -\nabla p + \frac{1}{Re_c} \nabla^2 \boldsymbol{u}. \tag{2}$$

The Reynolds number for the given centerline velocity is defined as $Re_c = U_{cl}h/\nu$, where ν is the kinematic viscosity of the fluid. Inner scales used to non-dimensionalize quantities are the friction velocity $u_\tau = \sqrt{\overline{\tau_w}/\rho}$ and the wall unit $\delta_\nu = \nu/u_\tau$, where ρ is the fluid density and $\overline{\tau_w}$ is the time- and area-averaged wall shear stress. Quantities non-dimensionalized by the inner scales are denoted with the usual superscript "+". The friction Reynolds number is then defined by $Re_\tau = u_\tau h/\nu = h/\delta_\nu$. For the current simulations, friction Reynolds numbers of $Re_\tau \approx 200, 500, 700$, and 1000 were considered. For this range of Reynolds numbers, the size of MFUs was $L_x \approx h$ and $L_z \approx 0.75h$, whereas for a typical extended domain, $L_x = 5h$ and $L_z = 3h$ were used. Simulations were performed using the opensource code Channelflow [30].

A numerical grid system was generated on $N_x \times N_y \times N_z$ (in x, y, and z) meshes, where a Fourier–Chebyshev–Fourier spectral discretization was applied to all field variables. The domain sizes used varied depending on the friction Reynolds number, but typical grid spacings used in the streamwise and spanwise directions were $\Delta x^+ \approx 7.5$ and $\Delta z^+ \approx 5$, respectively, for the range of Reynolds numbers studied in the MFUs. The nonuniform Chebyshev spacing used in the wall-normal direction of MFUs resulted in $\Delta y^+_{min} \approx 0.25$ at the wall and $\Delta y^+_{max} \approx 12$ at the channel center for the various Reynolds numbers studied. For the extended domains, streamwise and spanwise grid spacings were close to ones in MFUs. Grid system and resolution parameters are provided in Table 1. Note that the wall-normal spacing in the extended domains seems coarser, but it is still the same order as that used in the MFUs and other studies found in high-Reynolds-number literature [11,13]. A convergence check was also done—spatial resolution was increased and all the quantities reported in the current study were recalculated, yielding negligible changes from the results reported here. Each simulation run is sufficiently long (more than 20,000 h/U_{cl} time units) to ensure meaningful spatiotemporal averages.

The present study provides statistical information about the flow at increasing Reynolds numbers, with the goal of offering insights into the effect of periodic boundary conditions used in minimal flow units on MFU statistics and their connections to statistics of a sub-domain embedded within an extended domain. The sizes of the MFU domain were selected such that "healthy" turbulence was sustained. Healthy turbulence refers to the notion that the statistical properties of a flow are maintained and well represented by fundamental turbulent characteristics, even when using an MFU. Specifically, besides Jiménez and Moin [5], we also refer to healthy turbulence as when the friction Reynolds number saturates to its empirically predicted value and when flow statistics such as mean and fluctuating characteristics agree with those from extended domain simulations and experiments. Overly small domains can cause loss of fidelity in velocity fluctuations that may cause significant differences in flow structures, and subsequently, the statistical behavior of a flow, leading to unhealthy turbulence (see Section 3.2 for unhealthy cases).

Table 1. A summary of grid systems and resolutions for extended domain and minimal flow unit (MFU) simulations.

Re_τ	N_x	N_y	N_z	Δx^+	Δy^+_{min}	Δy^+_{max}	Δz^+
200 (MFU)	256 (64)	81 (121)	256 (84)	7.8 (6.2)	0.33 (0.13)	7.8 (6.4)	4.7 (2.2)
500 (MFU)	256 (86)	125 (161)	256 (84)	7.8 (5.2)	0.32 (0.17)	12.6 (8.8)	4.7 (4.0)
700 (MFU)	256 (86)	151 (181)	256 (102)	7.8 (6.9)	0.15 (0.24)	14.7 (12.0)	4.7 (4.7)
1000 (MFU)	256 (96)	191 (181)	256 (140)	7.8 (7.5)	0.14 (0.33)	16.5 (16.9)	6.3 (4.8)

3. Results

3.1. Minimal Flow Units up to $Re_\tau = 1000$

In adopting a similar approach to the MFU methodology [31,32], we fixed the domain length L_x and found the minimal domain width L_z that could sustain the turbulence. However, a larger L_x was sometimes needed if the flow relaminarized even with increasing L_z. As reported in the previous works [5,11], the minimum spanwise length that sustains turbulence

may be associated with an abnormality or unhealthy characteristics in mean velocity profiles, especially for higher Reynolds numbers (see Section 3.2 for details). To produce healthy turbulence in an MFU, the minimum domain size, especially in the spanwise direction, is chosen to ensure that the mean velocity profile collapses reasonably well with the logarithmic profile and that the wall shear stress agrees well with that of the extended domain. Figure 1 shows the MFU sizes for each Reynolds number studied. Figure 1a shows the maximum streamwise and spanwise wavelengths for each Reynolds number. The wavelengths in both streamwise and spanwise directions appear to increase linearly with Reynolds number. While these values are close to minimal values for sustaining healthy turbulence at these Reynolds numbers, it is possible to use smaller domains. For instance, while not explicitly enforced, the streamwise wavelength for all Reynolds numbers was larger than the spanwise wavelength for all cases. For a range of Reynolds numbers studied, smaller streamwise wavelengths could still allow for sustained healthy turbulence. Moreover, unlike the spanwise wavelength, changing the streamwise wavelength with the spanwise wavelength fixed seems to barely affect the healthiness of the turbulence. However, it should be noted that when the spanwise length $L_z^+ < 0.75 Re_\tau$, it caused MFU dynamics to become unhealthy for the Reynolds numbers studied (see Section 3.2 for details). Figure 1b shows the resultant area of the domain for each Reynolds number. Since both streamwise and spanwise wavelengths increase approximately linearly with Reynolds number, it is readily seen that the area increases in an approximately quadratic manner.
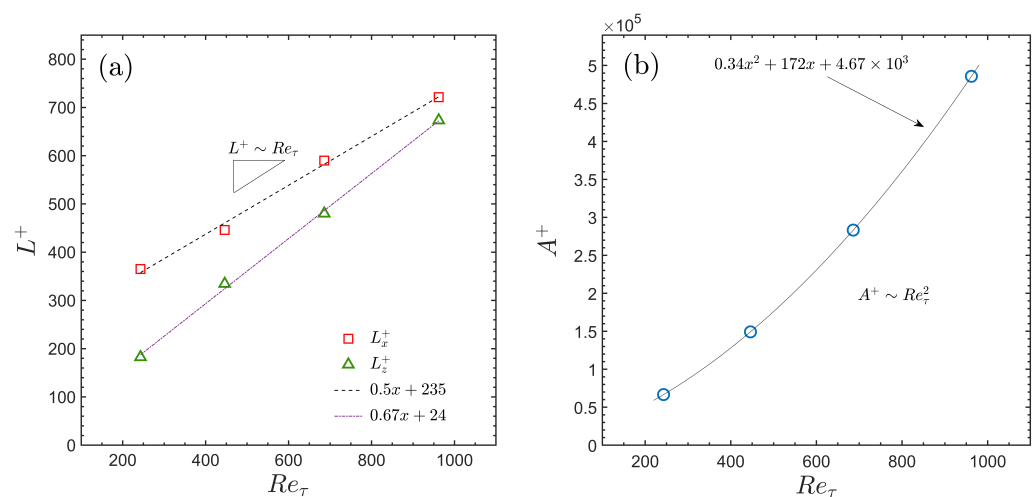

Figure 1. (**a**) The maximum streamwise and spanwise wavelengths for minimal flow units as functions of Reynolds number. Lines correspond to a linear fit. (**b**) Corresponding area $A^+ = L_x^+ \times L_z^+$ for each MFU as a function of Reynolds number. As expected, the solid line corresponds to a quadratic fit.

To ensure the healthiness of turbulent dynamics in MFU and sub-domain (SD) in an extended domain, Figure 2 shows a time series of area-averaged wall shear rates for both MFU and SD at each Reynolds number. It is clearly observed that there is good agreement between the two simulations for all Reynolds numbers, as the time series for the MFU and SD are nearly indistinguishable. As such, both mean and fluctuation characteristics agree quite well. To quantify this, the percent difference of the root-mean-square wall shear rates between MFU and SD was calculated. It is shown on the right of Figure 2 that for all Reynolds numbers, the percent difference (*r*) is less than 2%. It is also shown by power spectral density (not shown) that the most dominant frequencies of the wall shear stress are in good agreement between the MFUs and SDs.
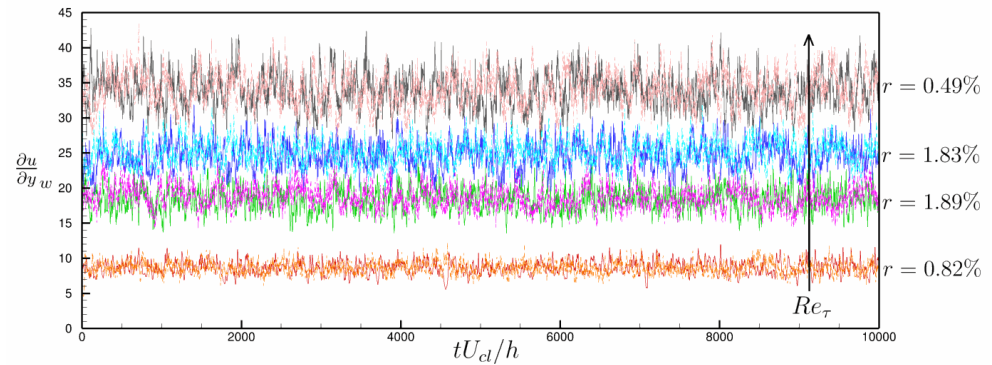
Figure 2. Time series of area-averaged wall shear rates for MFU (solid lines) and SD (dashed lines) in an extended domain at $Re_\tau = 200, 500, 700, 1000$. Both time series are nearly indistinguishable, indicating that mean and fluctuation characteristics agree quite well. Note that r is the percent difference of the root-mean-square wall shear rates between MFU and SD.

3.2. Healthiness of Minimal Flow Units

For the current MFU simulations, we used the minimum domain size that would sustain healthy turbulence. Figure 3 shows the effects of the streamwise and spanwise lengths on mean velocity profiles at $Re_c = 12,000$, $Re_c = 19,800$, and $Re_c = 28,800$. As seen in the figure, the streamwise length did not have a noticeable effect on the mean velocity profile at each Reynolds number. However, the spanwise length did have a significant effect when $L_z^+ < 0.75Re_\tau$. For $L_z^+ \approx 0.75Re_\tau$ at each Reynolds number, the mean velocity profile follows the Prandtl-von Kármán log law and shows a small deviation from the logarithmic profile around the channel center. Thus, it can still refer to healthy turbulence for this spanwise length. Note that for $L_z^+ > 0.75Re_\tau$, a slightly healthier mean velocity is visible around the channel center. It appears to suggest that it is reasonable to choose $L_z^+ \approx 0.75Re_\tau$ as an MFU spanwise length for the Reynolds numbers shown in Figure 3 when focusing on near-wall turbulence.
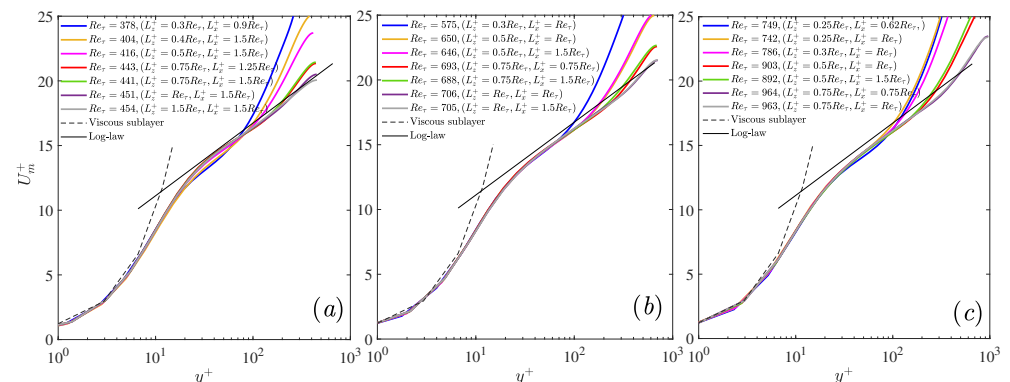

Figure 3. Healthy and unhealthy streamwise mean-velocity profiles for MFUs with various values of L_x^+ and L_z^+ at (**a**) $Re_c = 12,000$, (**b**) $Re_c = 19,800$, and (**c**) $Re_c = 28,800$. For these Reynolds numbers, when $L_z^+ < 0.75Re_\tau$, the mean velocity profiles appear to become unhealthy in regard to the logarithmic law.

For a decrease in the spanwise length from $L_z^+ \approx 0.75Re_\tau$, however, the MFU turbulence becomes unhealthy, as evidenced by a significant deviation of mean velocity profiles from the log law starting at $y^+ \sim O(100)$. As the spanwise length gets smaller, a deviation from the logarithmic law gets more severe. This unhealthy turbulence might stem from the fact that the small domain, particularly in the spanwise direction, fails to represent the large-scale coherent structures [11], which results in deteriorated turbulent characteristics despite no sign of relaminarization. However, it is worth mentioning that for Reynolds

numbers as small as $Re_c = 6000$ ($Re_\tau \approx 245$), reducing the domain size, particularly in the spanwise direction, is more likely to cause relaminarization [5]. In addition, a smaller domain size also causes an unrealistic reduction of wall shear stress and thus a smaller value of Re_τ for a fixed value of Re_c, as seen in Figure 3. By increasing the domain size, especially in the spanwise direction, the unrealistic reduction of wall shear stress can be avoided, which in turn increases Re_τ. Note that a further increase in a domain size from MFU size at a fixed Re_c does not lead to any noticeable change in Re_τ, which confirms the capability of the current MFU domain sizes to produce healthy turbulence. Nevertheless, unhealthy turbulence might be still observed for such small Reynolds numbers within tiny ranges of the spanwise length even with a saturated or correct Re_τ.

3.3. Mean Flow Properties

Figure 4 compares the mean streamwise velocity profiles for MFUs and SDs from different simulations at various Reynolds numbers. Regardless of Reynolds number or domain size, the profiles collapse agreeably onto the viscous sublayer and logarithmic profiles. Slight bumps are shown at the channel center for all simulations, which are reasonable [11]. One observation to note is the profile for the MFU at $Re_\tau = 200$ within the buffer region ($y^+ \approx 10$–30). It is slightly elevated not only compared to its SD counterpart, but also compared with all larger Reynolds number simulations. While the MFU profile for the rest of the channel agrees reasonably well with its SD counterpart and the log-law profile, similar anomalous behavior has been observed before in MFUs. It was found that for too small a domain size at $Re_\tau = 950$, a bump in a mean velocity profile was present near the channel center [33], and statistics above $y \approx L_z/3 \approx 0.25h$ were incorrect [6]. This resulted in an accelerated flow near the core of the flow. As the weak anomalous behavior in the present study was observed in the buffer layer at $Re_\tau = 200$, it may suggest that the domain size was too small to capture dynamics reliably. Additionally, the observed anomaly in the previous study was at a significantly larger Reynolds number [11]. To further test the log-law behavior, the inset in Figure 4 shows the diagnostic function of Ξ^+:

$$\Xi^+ = y^+ \frac{\partial U_m^+}{\partial y^+}, \tag{3}$$

which becomes constant and equal to the inverse of the von Kármán constant κ if the mean velocity profile displays a logarithmic layer. Aside from the obvious $Re_\tau = 200$ case, there are plateaus over a range within the log-law region, exhibiting logarithmic behavior. While the MFU diagnostic function near the core deviates from the SD values, there is good agreement between the two in the logarithmic region of the flow, suggesting MFU captures the mean behavior of the flow reasonably well. It should also be noted that despite a slight discrepancy in the log-law slope of $1/\kappa$, the von Kármán constant values are still within the reported range of 0.38–0.41 [11,13,34].

Figure 5 presents the mean-squared velocity fluctuations at the channel center. This quantity gives statistical information on the strength of velocity fluctuations at the core of the flow, which can also be used to compare differences in behavior between MFU and SD. The fluctuations at the centerline for MFU and SD are in good agreement for all Reynolds numbers. These values are also in good agreement with values shown by Lozano-Durán and Jiménez [11]. However, differences between MFU and SD are seen at low Reynolds numbers again, perhaps because the smaller domain size is too small to capture dynamics reliably. In addition, differences between the current study and Lozano-Durán and Jiménez (2014) could result from the same reason.
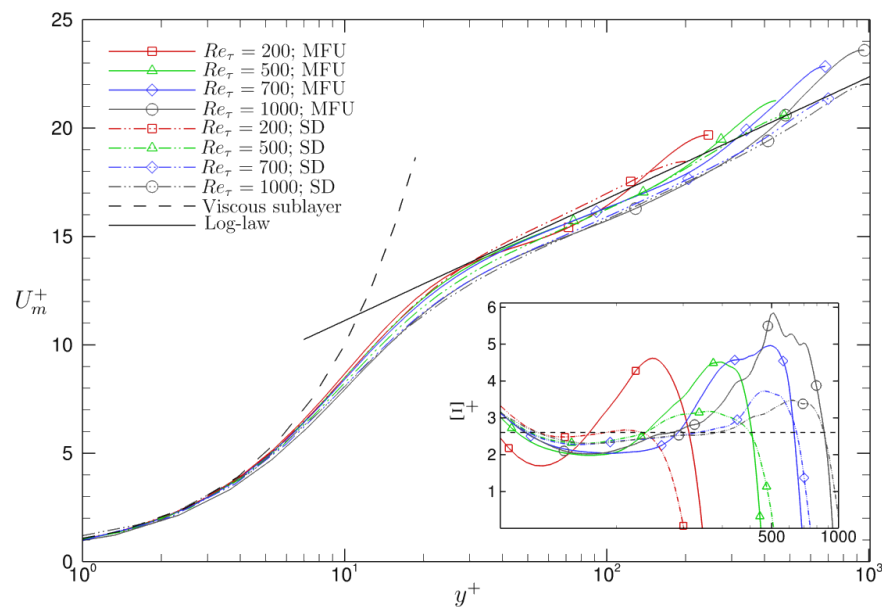
Figure 4. Mean velocity profiles for minimal flow units (MFU) and sub-domains (SD) for various Reynolds numbers along with the viscous sublayer and logarithmic law. Inset: Log-law diagnostic function Ξ^+. The dashed horizontal line is $1/\kappa$, where κ is the von Kármán constant and $\kappa = 0.384$.
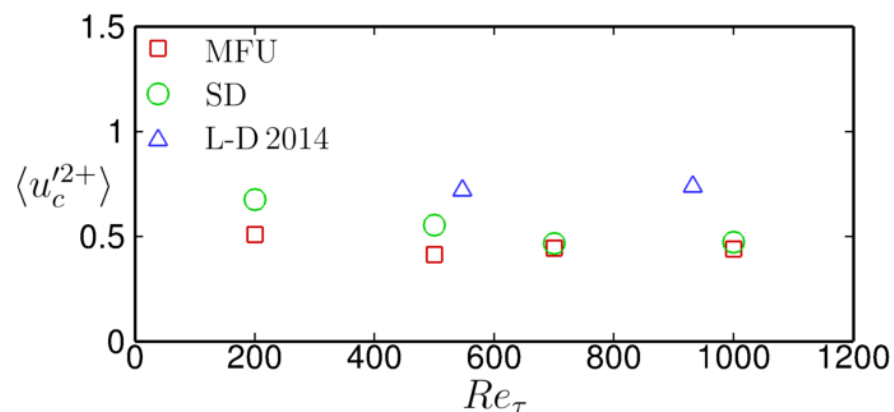

Figure 5. Mean-squared velocity fluctuations of minimal flow units (MFU) and sub-domains (SD) at the channel center for various Reynolds numbers. $\triangle$ are values obtained from Lozano-Durán and Jiménez [11] for larger domain simulations (L-D 2014).

3.4. Quadrant Analysis

Willmarth and Lu pioneered the use of Reynolds shear stress to describe the structure of turbulence in wall-bounded flows [26]. They utilized the so-called u'-v' plane to shed light on the notion of turbulent bursts, or short, infrequent spikes in turbulent kinetic energy observed in turbulent flows. This same style of analysis was applied here using joint probability density functions (JPDF) of the distributions of streamwise and wall-normal velocity fluctuations. Shown in Figure 6 are the JPDFs for the MFU and SD at each Reynolds number. These values were taken at a wall-normal plane at $y^+ \approx 30$.
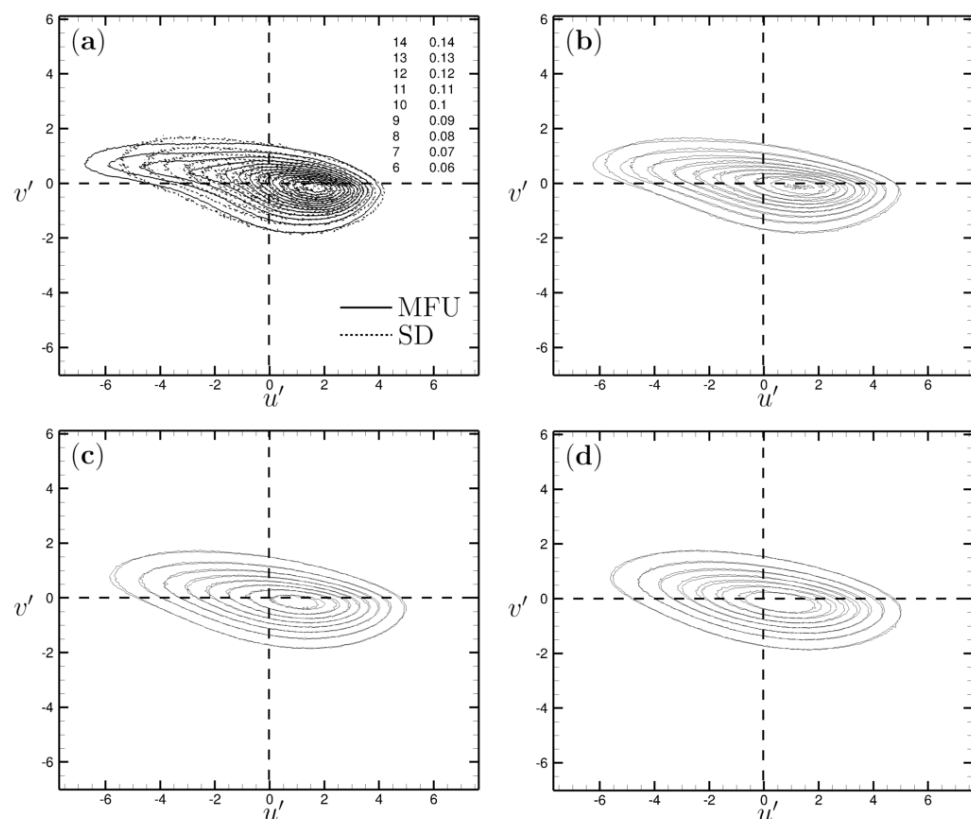
Figure 6. Contours of joint probability density functions for streamwise and wall-normal velocity fluctuations in a wall-normal plane at $y^+ \approx 30$ for MFUs (solid lines) and SDs (dashed lines) in an extended domain. Values were normalized by their respective friction velocities. $Re_\tau =$ (**a**) 200, (**b**) 500, (**c**) 700, and (**d**) 1000.

Overall, the shapes and levels of the distributions are in good agreement among the MFUs and SDs for all Reynolds numbers, showing almost no differences. This strongly suggests that MFU near-wall dynamics capture SD near-wall dynamics quite well. The majority of events occurred in quadrants Q2 and Q4, corresponding to ejections and sweeps, respectively, as was to be expected [35,36]. As the Reynolds number was increased, the distribution spread outward, and larger fluctuations were observed, which was also to be expected. For lower Reynolds numbers, it appears that the flow experienced more frequent and larger fluctuations along the negative u'-axis for MFU simulations. This is especially apparent for the MFU case at $Re_\tau = 200$, as there is a "tail" that formed in the Q2 quadrant corresponding to large negative u' fluctuations and small positive v' fluctuations. This same structure is not present in the JPDF in the SD data at $Re_\tau = 200$. This is in agreement with the trend seen in Figure 4 for the MFU at $Re_\tau = 200$, which resulted in a larger mean velocity. This discrepancy at $Re_\tau = 200$ could be explained by the fact that as the length scale of small-scale motions was found to be about 1000 wall units, an MFU domain was not sufficiently large to capture these small-scale motions at this Reynolds number [37]. For $Re_\tau = 700$ and 1000, however, the difference between the distributions of MFUs and SDs is negligible, as seen in Figure 6c,d, suggesting that MFU dynamics represent large-domain dynamics well up to $Re_\tau = 1000$.

4. Discussion

In this study, the effect of domain size on statistical behavior in a minimal flow unit (MFU) with periodic boundary conditions was investigated by direct numerical simulations up to $Re_\tau = 1000$. To accomplish this, the statistics from the MFU were compared with statistics from a sub-domain (SD) of the same dimensions as the MFU in an extended domain simulation. MFU dimensions were found by increasing the streamwise and

spanwise dimensions until turbulence was maintained and Re_τ saturated to its empirically predicted value. As one might expect, the minimal domain size necessary to meet these conditions increases with Reynolds number. Both streamwise and spanwise dimensions increase linearly with Reynolds number, and thus, the planar area increases in a quadratic manner. It was also found that when the spanwise length $L_z^+ < 0.75 Re_\tau$, MFU dynamics tended to become unhealthy for Reynolds numbers studied (see Figure 3).

Overall, there was good agreement between the wall shear rate dynamics and mean velocity profiles of MFU and SD simulations. Both MFU and SD profiles collapsed well onto the viscous sublayer and log-law profiles. These findings suggest that healthy MFU dynamics could represent more realistic extended-domain dynamics. The mean-squared streamwise velocity fluctuations at the centerline were also in good agreement, with MFU values slightly lower than their SD counterparts at lower Reynolds numbers. The values are slightly lower than those observed in previous extended domain simulations but are still agreeable [11].

A non-trivial finding was an observation that despite meeting these criteria for MFU (i.e., sustained turbulence and saturation of Re_τ), a simulation may still offer incorrect statistics in the bulk of the flow. While the behavior of the area-averaged wall shear rate was in great agreement for both MFU and SD, the mean velocity profile could still be incorrect. At $Re_\tau = 200$, this could be observed by the increase in the mean velocity profile in the buffer region of the MFU compared with all other simulations. There was also a distinct "tail" in the Q2 quadrant of the u'-v' JPDF, which was absent in the SD of extended domain simulations. This suggests that some additional criteria should be put in place to ensure healthy flow statistics when using MFUs.

Author Contributions: Conceptualization, S.M., E.A.D., and J.S.P.; methodology, J.S.P.; software, S.M. and E.A.D.; validation, S.M., E.A.D., and J.S.P.; formal analysis, S.M., E.A.D., and J.S.P.; investigation, S.M., E.A.D., and J.S.P.; resources, S.M. and E.A.D.; data curation, S.M. and E.A.D.; writing—original draft preparation, J.S.P.; writing—review and editing, S.M., E.A.D., and J.S.P.; visualization, S.M. and E.A.D.; supervision, J.S.P.; project administration, J.S.P.; funding acquisition, J.S.P. All authors have read and agreed to the published version of the manuscript.

Institutional Review Board Statement: Not applicable.

Informed Consent Statement: Not applicable.

Data Availability Statement: Data available on request from the authors.

Conflicts of Interest: The authors declare no conflict of interest.

Abbreviations

Abbreviations
The following abbreviations are used in this manuscript:

MFU	Minimal Fluid Unit
DNS	Direct Numerical Simulation
SD	Sub-Domain
JPDF	Joint Probability Density Function

References

1. Xi, L.; Graham, M.D. Active and hibernating turbulence in minimal channel flow of newtonian and polymeric fluids. *Phys. Rev. Lett.* **2010**, *104*, doi:10.1103/PhysRevLett.104.218301.

2. Hamilton, J.M.; Kim, J.; Waleffe, F. Regeneration mechanisms of near-wall turbulence structures. *J. Fluid Mech.* **1995**, *287*, 317–348, doi:10.1017/S0022112095000978.
3. Waleffe, F. On a self-sustaining process in shear flows. *Phys. Fluids* **1997**, *9*, 883–900, doi:10.1063/1.869185.
4. Agrawal, R.; Ng, H.C.H.; Davis, E.A.; Park, J.S.; Graham, M.D.; Dennis, D.J.; Poole, R.J. Low-and high-drag intermittencies in turbulent channel flows. *Entropy* **2020**, *22*, 1126.
5. Jiménez, J.; Moin, P. The minimal flow unit in near-wall turbulence. *J. Fluid Mech.* **1991**, *225*, 213–240.
6. Flores, O.; Jiménez, J. Hierarchy of minimal flow units in the logarithmic layer. *Phys. Fluids* **2010**, *22*, 071704.
7. Marusic, I.; Mathis, R.; Hutchins, N. High Reynolds number effects in wall turbulence. *Int. J. Heat Fluid Flow* **2010**, *31*, 418–428.
8. Hwang, Y. Near-wall turbulent fluctuations in the absence of wide outer motions. *J. Fluid Mech.* **2013**, *723*, 264–288.
9. Hwang, Y.; Bengana, Y. Self-sustaining process of minimal attached eddies in turbulent channel flow. *J. Fluid Mech.* **2016**, *795*, 708–738.
10. McKeon, B.J. The engine behind (wall) turbulence: Perspectives on scale interactions. *J. Fluid Mech.* **2017**, *817*, doi:10.1017/jfm.2017.115.
11. Lozano-Durán, A.; Jiménez, J. Effect of the computational domain on direct simulations of turbulent channels up to Reτ = 4200. *Phys. Fluids* **2014**, *26*, doi:10.1063/1.4862918.
12. Hoyas, S.; Jiménez, J. Scaling of the velocity fluctuations in turbulent channels up to Re_τ = 2003. *Phys. Fluids* **2006**, *18*, 011702.
13. Lee, M.; Moser, R.D. Direct numerical simulation of turbulent channel flow up to $Re_\tau \approx$ 5200. *J. Fluid Mech.* **2015**, *774*, 395–415, doi:10.1017/jfm.2015.268.
14. Lee, M.; Moser, R.D. Extreme-scale motions in turbulent plane Couette flows. *J. Fluid Mech.* **2018**, *842*, 128–145.
15. Kushwaha, A.; Park, J.S.; Graham, M.D. Temporal and spatial intermittencies within channel flow turbulence near transition. *Phys. Rev. Fluids* **2017**, *2*, doi:10.1103/PhysRevFluids.2.024603.
16. Wang, S.N.; Shekar, A.; Graham, M.D. Spatiotemporal dynamics of viscoelastic turbulence in transitional channel flow. *J. Non-Newton. Fluid Mech.* **2017**, *244*, 104–122, doi:10.1016/j.jnnfm.2017.04.008.
17. Podvin, B.; Lumley, J. A low-dimensional approach for the minimal flow unit. *J. Fluid Mech.* **1998**, *362*, 121–155, doi:10.1017/S0022112098008854.
18. Orlandi, P.; Pirozzoli, S.; Bernardini, M.; Carnevale, G.F. A minimal flow unit for the study of turbulence with passive scalars. *J. Turbul.* **2014**, *15*, 731–751, doi:10.1080/14685248.2014.927066.
19. Park, J.S.; Graham, M.D. Exact coherent states and connections to turbulent dynamics in minimal channel flow. *J. Fluid Mech.* **2015**, *782*, 430–454, doi:10.1017/jfm.2015.554.
20. Yin, G.; Huang, W.X.; Xu, C.X. Prediction of near-wall turbulence using minimal flow unit. *J. Fluid Mech.* **2018**, *841*, 654–673, doi:10.1017/jfm.2018.55.
21. Carlson, H.A.; Lumley, J.L. Active control in the turbulent wall layer of a minimal flow unit. *J. Fluid Mech.* **1996**, *329*, 341–371, doi:10.1017/S0022112096008944.
22. Xi, L.; Graham, M.D. Intermittent dynamics of turbulence hibernation in Newtonian and viscoelastic minimal channel flows. *J. Fluid Mech.* **2012**, *693*, 433–472, doi:10.1017/jfm.2011.541.
23. Davis, E.A.; Park, J.S. Dynamics of laminar and transitional flows over slip surfaces: Effects on the laminar-turbulent separatrix. *J. Fluid Mech.* **2020**, *894*, doi:10.1017/jfm.2020.282.
24. Wei, T.; Willmarth, W.W. Reynolds-number effects on the structure of a turbulent channel flow. *J. Fluid Mech.* **1989**, *204*, 57–95, doi:10.1017/S0022112089001667.
25. Jiménez, J.; Pinelli, A. The autonomous cycle of near-wall turbulence. *J. Fluid Mech.* **1999**, *389*, 335–359.
26. Willmarth, W.W.; Lu, S.S. Structure of the reynolds stress near the wall. *J. Fluid Mech.* **1972**, *55*, 65–92.
27. Lu, S.S.; Willmarth, W.W. Measurements of the structure of the Reynolds stress in a turbulent boundary layer. *J. Fluid Mech.* **1973**, *60*, 481–511, doi:10.1017/S0022112073000315.
28. Lu, S.S.; Willmarth, W.W. Measurement of the mean period between bursts. *Phys. Fluids* **1973**, *16*, 2012–2013, doi:10.1063/1.1694249.
29. Willmarth, W.; Lu, S. Structure of the Reynolds Stress and the Occurrence of Bursts in the Turbulent Boundary Layer. In *Turbulent Diffusion in Environmental Pollution*; Frenkiel, F., Munn, R., Eds.; Academic Press: Cambridge, MA, USA, 1975; Volume 18, pp. 287–314, doi:10.1016/S0065-2687(08)60467-7.
30. Gibson, J.F. Channelflow: A Spectral Navier-Stokes Simulator in C++. Technical Report, U. New Hampshire, 2012. Available online: Channelflow.org (accessed on 19 April 2021).
31. Xi, L.; Graham, D.M. Turbulent drag reduction and multistage transitions in viscoelastic minimal flow units. *J. Fluid Mech.* **2010**, *647*, 421.
32. Wang, S.N.; Graham, M.D.; Hahn, F.J.; Xi, L. Time-series and extended Karhunen—Loève analysis of turbulent drag reduction in polymer solutions. *AIChE J.* **2014**, *60*, 1460–1475.
33. Jiménez, J. How linear is wall-bounded turbulence? *Phys. Fluids* **2013**, *25*, 110814, doi:10.1063/1.4819081.
34. Smits, A.J.; McKeon, B.J.; Marusic, I. High-Reynolds number wall turbulence. *Annu. Rev. Fluid Mech.* **2011**, *43*, 353–375.
35. Antonia, R. Conditional sampling in turbulence measurement. *Annu. Rev. Fluid Mech.* **1981**, *13*, 131–156.
36. Wallace, J.M. Quadrant analysis in turbulence research: history and evolution. *Annu. Rev. Fluid Mech.* **2016**, *48*, 131–158.

37. Lee, M.; Moser, R.D. Spectral analysis of the budget equation in turbulent channel flows at high Reynolds number. *J. Fluid Mech.* **2019**, *860*, 886–938.